**CAV2021**
11th International Symposium on Cavitation
May 10-13, 2021, Daejon, Korea

# NUMERICAL SIMULATION OF CAVITATING FLOW PAST A CYLINDRICAL PIN LOCATED AT THE THROAT OF A VENTURI

Mohit Kannan[1]* and Dhiman Chatterjee[1]

[1]Department of Mechanical Engineering
IIT Madras, Chennai 600036, INDIA

**Abstract:** Cavitating flow, over a circular cylinder in cross-flow, is numerically simulated for different Reynolds number spanning the subcritical flow regime. It is known that the occurrence of cavitation influences the flow features and impacts drag experienced by a cylinder. Reynolds number and blockage factor are known to influence cavity formation and dynamics. Another factor that may become important is the influence of neighbouring walls as given by the gap parameter. Numerical simulations are carried out using OpenFOAM for a 3D planar venturimeter with a small cylindrical pin at the centre of the throat of the venturi and oriented perpendicular to the flow. Aspect ratio is 2.67, blockage factor is 20%, and the gap parameter is 2.5. The effects of cavitation on drag and cylinder surface pressure coefficient as well as static pressure, void fraction, and turbulent kinetic energy are presented.

**Keywords:** shear layer cavitation; cylinder; upper subcritical flow

## 1. Introduction

Shear layer cavitation is the formation of cavities in zones of high shear and turbulent fluctuations such as in the core of the vortices. Typically, a turbulent shear layer contains spanwise (primary) and streamwise (secondary) vortices as confirmed by the studies of [1]. Sumer and Fredsoe [2] have divided turbulent flow past a circular cylinder into subcritical ($300< Re_D <3 \times 10^5$), critical/lower transition ($3 \times 10^5< Re_D<3.5 \times 10^5$), supercritical ($3.5 \times 10^5< Re_D <1.5 \times 10^6$), upper transition ($1.5 \times 10^6< Re_D<4 \times 10^6$), and transcritical ($Re_D>4 \times 10^6$), where $Re_D = \frac{U_{throat} d}{\nu}$ is the Reynolds Number based on the cylinder diameter (d), velocity at the throat of the venturi ($U_{throat}$), and fluid property ($\nu$).

Upper subcritical flow ($20k \leq Re_D \leq 300k$) is characterized by an attached laminar boundary layer, a turbulent wake, and the occurrence of transition in the shear layer. Depending on the Re, inception may occur on the surface of the cylinder, in the shear layer, or the wake. Wykes [3] studied the cavity formation for different flow regimes and concluded that, for the subcritical flow regime, the cavity inception took place in the shear layer or wake whereas, for the critical flow regime, inception took place on the cylinder surface.

Ramamurthy and Bhaskaran [4] studied the effect of blockage on cavitating flow past a circular cylinder and observed that the wall interference effect was less at high $\sigma$ but at low $\sigma$ this effect was high and there was a sharp drop in drag coefficient ($C_D$) with a reduction in $\sigma$. In a recent study, Sahu et al. [5] brought out the effect of blockage on cavitation in the near-wake of a bigger-sized cylinder (diameters varied between 9 mm and 30 mm and length of 150 mm). In these experiments, 5≤aspect ratio (AR)≤ 16.67, 6% (unblocked case) ≤blockage factor (BF) ≤ 20%, and 2.5 ≤gap parameter (GF) ≤8.3.

Gnanaskandan and Mahesh [6] investigated the wake characteristics behind a circular cylinder under cavitating conditions using a homogeneous mixture model at very low Re. They noticed that cavitation suppressed turbulence and delayed the 3D breakdown of Kármán vortices.

*Corresponding Author: Mohit Kannan, mohitkannan007@gmail.com

A review of the existing literature reveals the scarcity of works done in studying the flow past a circular cylinder under cavitating conditions, particularly in upper subcritical flows. The motivation for the present work is to address this gap by studying the dynamics of the shear layer in the wake of a cylindrical pin at four cavitation numbers and three $Re_D$. The numerical investigations were carried out using the open-source code software OpenFOAM.

## 2. Computational Details

### 2.1. Solver Details

interPhaseChangeFoam with phase-change was used to simulate the unsteady turbulent cavity in the shear layer of the cylinder. The solver is based on Transport Equation Model (TEM) and hence solves a single momentum equation for the phase mixture. Turbulence closure was achieved using the k-ω SST model. For brevity, governing equations for mass and momentum as well as turbulence model are not described here. We have used the Kunz [7] formulation for the source term which employs different strategies to compute the evaporation and condensation terms. The transformation from liquid to vapour (evaporation) is computed as being proportional to the amount by which the pressure is below the vapour pressure whereas the transformation from vapour to liquid (condensation) is modeled using a cubic polynomial, based on the liquid volume fraction.

### 2.2. Numerical Setup

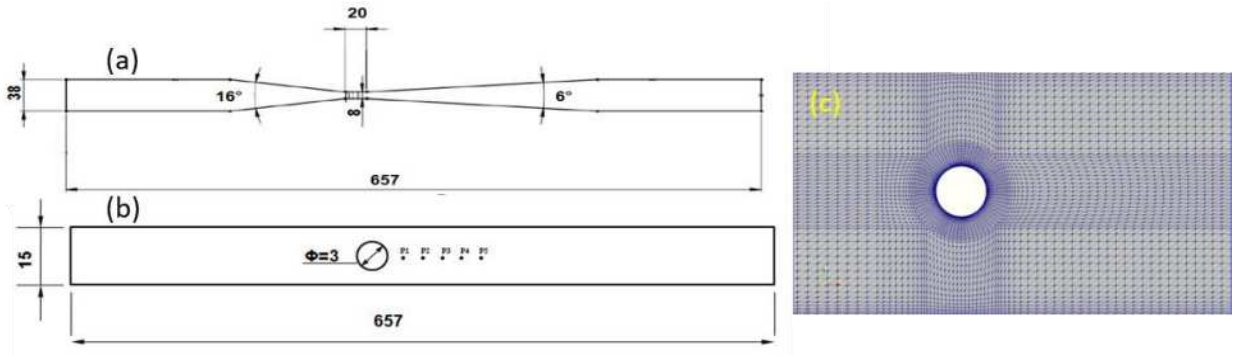


**Figure 1.** Schematic of the computational domain (a) is the front view and (b) is the top view of the domain. $P_1$ to $P_5$ shows the axial location of probes at a fixed distance of 0.5d. (c) Zoomed view of High-resolution O-grid near the cylinder. All dimensions are in mm.

The computational domain is shown in Figure 1. The height of this 3D planar venturimeter varies from an inlet height of 38 mm to 8 mm at the throat. In this geometry, the same BF (20%) and GF (2.5), as given in the paper by Sahu et al. [5], are maintained while AR (2.67) is significantly reduced. A structured mesh shown in Fig 1 (c) was built in ICEM-CFD to obtain a wall y+=1. A mesh with 1.28 million elements, obtained after the grid independence study was used for all the simulations. At the inlet, a velocity boundary condition, and at the outlet, a pressure boundary condition was imposed. No-slip boundary condition was used for walls. Unsteady simulations were carried out till the initial transience decayed before carrying out the statistical analysis. The pressure-velocity coupling was realized by implementing PIMPLE algorithm where a SIMPLE (Semi-Implicit Method for Pressure-Linked Equation) outer-corrector loop is coupled with a PISO (Pressure Implicit with Splitting of Operators) inner-corrector loop. The spatial derivatives were computed using a second-order upwind scheme and Van Leer scheme was

*Corresponding Author: Mohit Kannan, mohitkannan007@gmail.com

used in the advection of the volume fraction function. Courant number for all the simulations were maintained below 0.5.

### 3. Results

The inception of cavitation was seen to occur at σ=3.785, which is close to that obtained by [5]. Fig 2 shows instantaneous contours of water fraction and corresponding contours of turbulent kinetic energy at the same time instants. The water contours show the presence of shear layer cavitation for all Reynolds number at σ=2.898. However, at a lower cavitation number (σ=2.012), typical instantaneous contours show a very different nature. The turbulent kinetic energy contour indicates to be high in those locations where cavities are close to end.

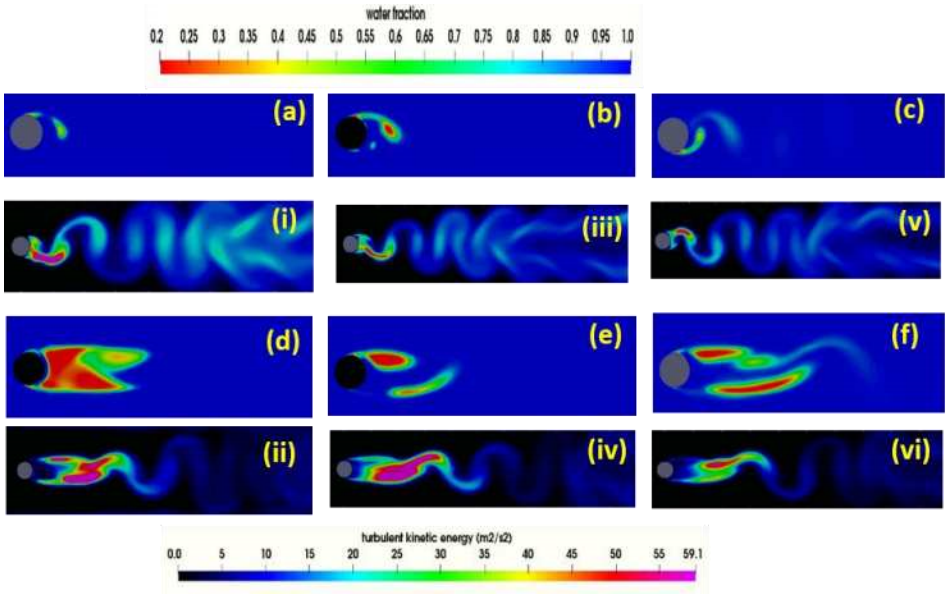


**Figure 2.** (a-f) represents typical instantaneous water fraction contours. (a),(b),(c) are contours at σ=2.898 and (d),(e),(f) are contours at σ=2.012 for Re=14k (a, d), 70k (b, e) and 350k (c, f) respectively. (i-vi) are instantaneous turbulent kinetic energy (T.K.E.) contours shown at the same time instants of water fraction (a-f). (i),(ii) are T.K.E. at Re=14k; σ=2.898 and σ=2.012 respectively; (iii),(iv) are T.K.E. at Re=70k; σ=2.898 and σ=2.012 respectively and (v),(vi) are T.K.E. at Re=350k; σ=2.898 and σ=2.012 respectively.

The validation for the present study is carried out by comparing the mean pressure coefficient over the cylinder surface $\overline{C_P} = \frac{P_\theta - P_{Throat}}{\frac{1}{2}\rho U_{Throat}^2}$ with the experimental values of [5] and a reasonable agreement in the trend was found as evident from Figure 3(a). The pressure distribution indicates that the flow separates at around 80°, which confirms the existence of a laminar boundary layer upstream of separation. Figure 3(b) shows a decrease in the mean drag coefficient due to cavitation. This happens because of the formation of the cavity downstream of the cylinder.

Fig 4(a) shows the variation of mean vapour fraction for different cavitation number at Re=14k. It shows the peak of vapour fraction occurs at one diameter distance downstream of the cylinder center. Fig 4(b) shows the variation of turbulent kinetic energy for different Reynolds number for σ=2.898. It shows that the peak of turbulent kinetic energy (TKE) occurs at a location slightly downstream of the peak of vapour fraction, thereby indicating that the peak in TKE to be related to the collapse of the cavity.

*Corresponding Author: Mohit Kannan, mohitkannan007@gmail.com

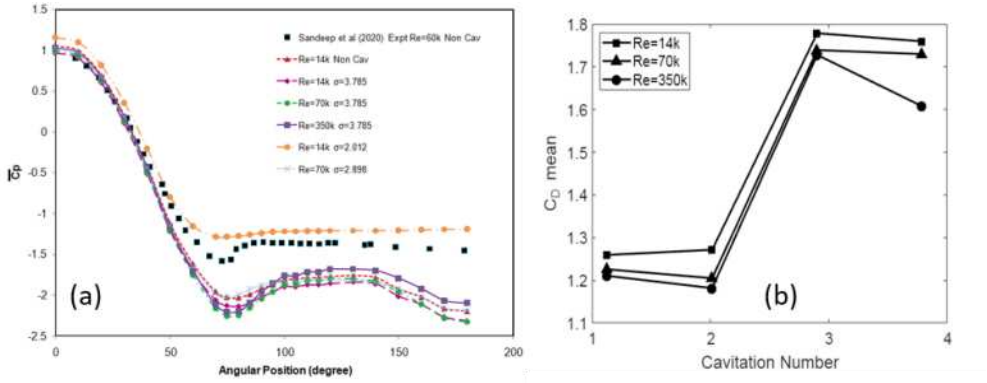


**Figure 3.** (a) Variation of mean pressure coefficient on the cylinder surface $\overline{C_P}$ for different $Re_D$ and cavitation number. (b) Mean drag coefficient vs cavitation number for different $Re_D$.

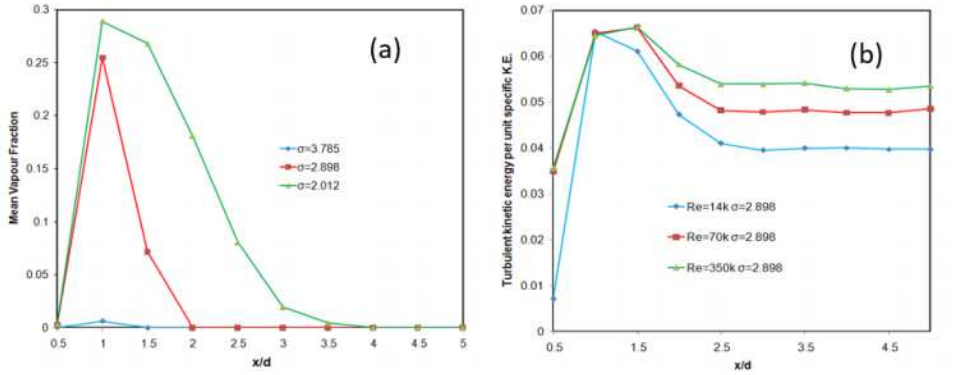


**Figure 4.** (a) Mean vapour fraction vs x/d for different cavitation number at $Re_D$=14k. (b) Turbulent kinetic energy (TKE) per unit specific kinetic energy vs x/d for different $Re_D$ at σ=2.898.

**Acknowledgments:** The authors acknowledge P.G. Senapathy Center for Computing Resources, Indian Institute of Technology Madras for providing the necessary computational facility.

## References

1. Ooi, K. K.; Acosta, A. J. (1983). *The utilization of specially tailored air bubbles as static pressure sensors in a jet.*Trans. ASME I: J. Fluids Eng.106, 459-465.
2. Sumer, B. M.; Fredsoe J.(2006). *Hydrodynamics around cylindrical structures*. World Scientific Publishing Ltd., Singapore.
3. Wykes, M. E. P. (1978). *Experimental studies of viscous effects on cavitation*. Ph.D. thesis, St. John's College, University of Oxford, United Kingdom.
4. Ramamurthy, A.; Bhaskaran P. (1977). *Constrained flow past cavitating bluff bodies.* ASME J. Fluids Eng., 99, 717–726.
5. Sahu et al. (2020).*Investigation of the blockage effect on flow past a circular cylinder*. Interfacial Phenomena and Heat Transfer, 8(2), 93-105.
6. Gnanaskandan, A.; Mahesh K.(2016). *Numerical investigation of near-wake characteristics of cavitating flow over a circular cylinder*. J. Fluid Mech, 790, 453–491.
7. Kunz, R. F. et al. (2000). *A preconditioned Navier Stokes method for two-phase flows with application to cavitation prediction.* Computational Fluids, 29, 849875.

*Corresponding Author: Mohit Kannan, mohitkannan007@gmail.com